Noble Gases Deliver Cool Dates from Hot Rocks

Cécile Gautheron[1] and Peter K. Zeitler[2]

ABSTRACT

Heat transfer in the solid Earth drives processes that modify temperatures, leaving behind a clear signature that we can measure using noble gas thermochronology. This allows us to record the thermal histories of rocks and obtain the timing, rate, and magnitude of phenomena such as erosion, deformation, and fluid flow. This is done by measuring the net balance between the accumulation of noble gas atoms from radioactive decay and their loss by temperature-activated diffusion in mineral grains. Together with knowledge about noble gas diffusion in common minerals, we can then use inverse models of this accumulation–diffusion balance to recover thermal histories. This approach is now a mainstream method by which to study geodynamics and Earth evolution.

KEYWORDS: geochronology, thermochronology, diffusion, noble gas geochemistry

INTRODUCTION

Temperature matters to geologists. Heat transfer within our dynamic planet drives deformation of the lithosphere and the development of topography, which, in turn, drives erosion and other surface processes (FIG. 1). Changing temperature alters rock properties, controlling crustal behavior during deformation. And processes such as erosion, sedimentation, magmatism, and fluid flow can interact and modify temperatures in the crust. At plate boundaries and within continental interiors, growth and erosion of high mountains and plateaus divert atmospheric circulation, leading to feedbacks that integrate the solid Earth with surface processes, leaving behind a record of rocks with diagnostic temperature histories.

Using temperature-sensitive dating methods applied to a variety of minerals, we can measure such temperature changes, which can then be used to understand the timing and magnitude of geodynamic processes and the role of the solid Earth within the Earth system. Those dating methods, which most commonly rely on the accumulation of the

---

1 Université Paris-Saclay, CNRS, GEOPS
91405, Orsay, France
E-mail: cecile.gautheron@universite-paris-saclay.fr
[2] Department of Earth and Environmental Sciences
Lehigh University
Bethlehem, PA, 18015, USA
E-mail: peter.zeitler@lehigh.edu

radiogenic gasses ^{4}He or ^{40}Ar and are balanced by gas loss via temperature-activated diffusion, form part of the subdiscipline known as thermochronology. Also, in this subdiscipline, but not covered in this issue, is fission track thermochronology, which relies on the accumulation and temperature-activated annealing of damage 'tracks' produced by ^{238}U fission. By combining our understanding of diffusion behavior in minerals with models of noble gas accumulation and loss, we can infer thermal histories from measured ages. In terrestrial applications, the temperature sensitivity of noble gas thermochronology spans conditions from the middle- to upper crust, ideal for studying tectonics, geomorphology, basin analysis, and more. The other articles in this issue provide specific examples of how this approach can help to solve exciting and important geological problems on Earth and beyond.

Excellent reviews of the origins and underpinnings of thermochronology already exist (McDougall and Harrisson 1999; Reiners et al. 2005, 2018; Ault et al. 2019). Here, we highlight thermochronology's fundamental principles and how knowledge about noble gas diffusion behavior provides an opportunity to learn about the evolving Earth.

HISTORY

The field of geochronology was developed in the early 20th century. But it became increasingly obvious that mineral ages measured using different methods often disagreed and were younger than geological constraints. In the 1960s, workers reached the key conclusion that this apparent unreliability was actually a useful consequence of a sample's temperature history. This set the stage for Martin Dodson's introduction of the concept of closure temperature (Dodson 1973), which changed the course of geochronology by showing how to use diffusion theory to quantify mineral-age interpretation. It became the expectation (rather than a surprise) that different minerals from a single rock should give different ages. Dodson's work encouraged subsequent generations of geochemists to apply diffusion theory to age data.

Mark Harrison (currently at University of California, Los Angeles, USA) catalyzed the use of noble gas thermochronology for terrestrial applications in a series of papers that exploited the new ^{40}Ar/^{39}Ar method, showing how quantitative, diffusion-based analysis of argon mineral ages could be applied to settings such as orogens, basins, and intrusive contacts (MacDougall and Harrison 1999). The previously dismissed U–Th/He method was resurrected by Zeitler et al. (1987), and there was a series of papers by Ken Farley's group at the California Institute of Technology (USA) (e.g., Farley 2000), all of which led to the development of dating approaches suited to low-temperature processes (<250 °C). The ^{40}Ar/^{39}Ar and ^{4}He/^{3}He step-heating methods were developed to reveal continuous thermal-history information rather than single time–temperature points. And from this, additional means of reconstructing thermal histories were developed based on how radiation damage can alter helium diffusion (Shuster et al. 2006; Flowers et al. 2009; Gautheron et al. 2009; Guenthner et al. 2013). Finally, spurred by wide interest in applying these methods to geologic problems, inverse models were developed to rigorously extract the thermal histories recorded by observations (Ketcham 2005; Gallagher 2012) and to also assess the geodynamic significance of these thermal histories in constraining processes like erosion, subsidence, faulting, and landscape evolution (e.g., Braun 2003).

HOW NOBLE GAS THERMOCHRONOMETERS WORK

Thermochronology differs from geochronology because it embraces situations where radioactive decay systems are not closed, but open: there is diffusive loss of the daughter product. Understanding thermochronological methods, thus, requires an understanding of both noble gas geochronology and the diffusion behavior of noble gases in minerals.

Accumulation by Radioactive Decay

Noble gas geochronology is based on the production of noble gas daughters through a variety of mechanisms: decay of ^{40}K to ^{40}Ar; decay of ^{238}U, ^{235}U, ^{232}Th, and ^{147}Sm to alpha particles that become ^{4}He atoms; nucleogenic interaction of alpha particles with crystal atoms to produce ^{20,21,22}Ne (and even ^{84}Kr); and radiogenic production of ^{129,131,136}Xe by spontaneous fission of ^{238}U and radioactive decay of iodine. We will focus on methods involving He and Ar (FIG. 2). Although the decay rates for ^{40}K and the ^{4}He parent isotopes are not high, noble gases are easy to precisely measure across time scales from thousands to billions of years. Moreover, the U and Th decay chains release 6 to 8 helium nuclei in the form of alpha particles (only one alpha particle is produced during Sm decay), amplifying ^{4}He production rates. Finally, argon and helium are highly incompatible elements and have low solubility in minerals, so very little is incorporated at the time of mineral formation.

The main difference in how K–Ar and U–Th/He measurements are handled is mostly methodological. First, because Earth's atmosphere is ~1% argon, it is necessary to correct for ^{40}Ar contamination, usually by measuring stable ^{36}Ar and using the atmospheric ^{40}Ar/^{36}Ar ratio. In contrast, because of its low atmospheric concentration, correction for initial ^{4}He is unnecessary. Second, during decay, ^{40}Ar and ^{4}He atoms travel some distance before stopping. For argon, this short distance can be neglected; but for helium, the distance varies from 5 μm to 30 μm (FIG. 2), requiring an alpha-ejection correction for decays that happen close to grain margins. Finally, another practical difference between Ar and He chronometers is that K occurs at percent levels in commonly used minerals such as feldspars, micas, and amphiboles, whereas U and Th occur at ppm levels in accessory phases such as apatite, zircon, and titanite.

Loss by Diffusion

Being chemically inert and present in small amounts, noble gases in minerals act as ideal tracer diffusants. Atoms diffuse between neighboring sites following a 3-D random walk within the host crystal structure. The differences in diffusion rate for noble gases in minerals are linked to atomic size and the energy required to jump between sites (Farley 2000). Diffusion jump distances lie close to the size of the unit cell, which means that to escape from a small grain using a random walk, a noble gas atom follows a path several *meters* in length! This implies that diffusing atoms visit large fractions of each grain's volume, guaranteeing interaction with imperfections in the crystal lattice. Whereas individual diffusing atoms take random walks, the ensemble diffusion of many atoms emerges as a smooth profile that leaves a grain with high interior concentrations that decrease towards the zero-concentration boundary at its edge (FIG. 2).

However, just knowing about diffusion mechanisms is not enough. For thermochronology, we need to know how diffusion rates depend on temperature, and we need to know several other factors specific to the mineral grain in which we measure the noble gases. Diffusion in a crystal lattice typically obeys an exponential temperature dependence described by the Arrhenius equation: diffusion kinetics for each noble gas in each mineral grain are characterized by an activation energy E_a and a diffusivity at infinite temperature D_o. The diffusion dimension must also be known—in some cases this is the actual grain size (noted as a or r); in others, it is a smaller domain defined by crystallographic structures (FIG. 2).

How do we know the real diffusion parameters? Our knowledge is based on a fairly limited database of laboratory diffusion experiments, although for a few thermochronometers, kinetic information can be obtained as part of the analysis process. Diffusion experiments can be performed using natural ^{4}He or ^{40}Ar, or better, using uniformly distributed ^{3}He or ^{39}Ar created from proton spallation or fast-neutron reactions with the sample's constituent atoms (McDougall and Harrison 1999; Shuster and Farley 2004). Using these artificial isotope profiles as a reference, progressive step-heating analysis can reveal the internal distribution of ^{4}He or ^{40}Ar and, thus, information about a sample's specific kinetics (FIG. 2). An obvious issue is that kinetic experiments occur over laboratory timescales that are a billion times shorter than geologic applications. Therefore, an important supplement to our kinetic calibrations for various thermochronometers comes from numerous comparative studies where the performance of different systems can be compared with one another in geologic settings having well-understood temperature histories.

Compared to idealized "perfect crystals", diffusion behavior in real samples—as shown by *ab initio* calculations (e.g., Djimbi et al. 2015) and laboratory experiments—is complicated by imperfections that are the result of chemical substitutions, strain-induced defects, radiation damage, or voids in the structure (including fluid inclusions). Noble gas diffusion can be accelerated if the imperfection content is high enough to provide many fast paths, but, more commonly, at lower levels, damage will slow diffusion due to trapping or obstruction of diffusion pathways. For example, diffusion experiments show how different natural apatite crystals from the same sample can be characterized by different diffusion behaviors and that He within some apatite crystals can occur in different sites, such as within the crystal lattice, defects, damage zones, and/or voids (McDannell et al. 2018) (FIG. 3).

Net Retention Behavior

Dodson (1973) set out the mathematics needed to describe the balance between radiogenic production and diffusional loss. For cooling systems, this leads to the concept of *closure temperature (T_c),* which gives *the temperature of the system at the time given by the measured age* (FIG. 4). This insight provided a quantitative framework for thermochronology: under the right conditions, a sample's differing ages can be interpreted as a series of time–temperature points along its thermal history. Thus, above T_c, noble gases produced by decay will be completely lost by diffusion, while below T_c those gases will be fully retained. During cooling at temperatures close to T_c, only some noble gas atoms will be retained.

Closure temperature depends on a specific sample's diffusion dimension and cooling rate, as well as its individual kinetics (FIG. 4). As a practical matter, it is worth knowing that in comparing different systems, people often cite a single value for T_c, which is referenced to a slow cooling rate of 10 °C/My and a "typical" grain size. If a rock undergoes a pulse of reheating after cooling, the noble gas atoms accumulated in the crystal can be partially or totally lost, and this will "reset" the system. This can happen for a wide range of time and temperature combinations. It is important to realize that closure temperature *cannot* be equated to an "opening" temperature.

Closure temperature is a crucial concept, but many geological processes involve more than just cooling at a constant rate—in general, a thermochronometer age could be the outcome of myriad variations of thermal history. For thermal histories where a rock spends many millions of years teetering at near-constant temperatures where argon or helium are partially retained, if there are major changes in cooling rate, or if reheating and partial resetting come into play, the concept of simple closure temperature does not apply, even if the measured age still represents a net measure of the sample's complex history. As we discuss below, this is why modeling is an important aspect of thermochronological analysis.

Thermochronometers

Numerous systems are now available for use in geological applications. FIGURE 4 compares these thermochronometers and their temperature ranges.

Helium

Most U–Th/He thermochronology uses the accessory minerals apatite and zircon, which are common in many rock types. This system can address the low temperatures of 40–120 °C (by apatite) and <100–200 °C (by zircon). Titanite and rutile have seen some use, and successful dates have also been obtained on fluorite, goethite, hematite, magnetite and spinel. But, for all these systems, more diffusion data are needed. In many cases, single grains are analyzed for total U, Th, Sm, and He concentrations, yielding a single age. In some cases, ^{4}He/^{3}He analysis is used for apatite. Though more time-intensive, this approach allows stepwise heating to measure sample-specific diffusion kinetics and learn more about the sample's thermal history (FIG. 2).

For apatite, zircon, and titanite, the diffusion domain is the dated grain itself. Radiation damage strongly impacts on He diffusion, leading to a broad spread of temperature sensitivity (FIG. 4) and, often, a correlation between (U–Th)/He age and effective uranium (eU), or the concentration of U and Th weighted for their alpha productivity (e.g., FIG. 2). For polycrystalline phases such as hematite, variable retentivity is controlled by the range in diffusion dimensions (FIGS. 2 and 4) (Cooperdock and Ault 2020 this issue).

Argon

The minerals most commonly used for argon-based thermochronology are K-feldspar, biotite, the white micas, and the amphiboles (FIG. 4). Essentially all analyses use the ^{40}Ar/^{39}Ar variant of the K–Ar method, a form of neutron activation analysis for K that allows age information to be determined directly from ^{40}Ar/^{39}Ar data, through the use of suitable age standards (FIG. 2). Step-heating analysis can reveal ^{40}Ar concentration gradients and can also use ^{39}Ar loss to obtain sample-specific kinetic data. Together, these data can be inverted for thermal histories (see below). In practice, the observed instability of ferromagnesian hydrous phases under vacuum means that step-heating results from biotite and amphibole do not yield useful kinetic data. As a result, step heating is most fruitful when used with feldspars and white micas. These latter phases have been shown to be stable, or at least metastable, during heating.

Because feldspars remain stable during vacuum heating, considerable effort has gone into the development of K-feldspar ^{40}Ar/^{39}Ar thermochronology based on the multi-diffusion domain (MDD) model (Lovera et al. 1991). This posits that intragrain features reduce diffusion dimensions to be much smaller than the physical grain size. FIGURE 4 shows how MDD behavior alters and extends thermal sensitivity and how the thermal history can be obtained by inverse models. Although most MDD analyses have been on K-feldspar, muscovite appears to show MDD behavior as well. Plagioclase holds some promise, but data interpretation is more complicated because of much lower K contents and complex zoning.

Potential Complications

Argon- and helium-based thermochronometers can be impacted by a variety of phenomena. Zoning of U–Th in some minerals will complicate alpha-ejection correction, and U–Th or K zoning will alter He or Ar diffusion processes. Samples need to be fresh, unaltered, pure phases in which diffusion was the main transport mechanism. Despite great interest in the thermal history of shear zones, this is a challenging geochemical environment: there can be extensive flow of fluids containing ^{40}Ar and ^{4}He, and dynamic recrystallization can lead to the development of crystallographic defects. Metamorphic and hydrothermal fluids can also paint thin layers of U-rich phases around grains, leading to implantation of excess ^{4}He that can be significant for low-U phases. Also, fluid inclusions and partitioning into retentive sites can cause minerals to incorporate nonradiogenic “excess” ^{40}Ar or ^{4}He. Such problems are not widespread, but care must be taken to anticipate and, if possible, avoid them.

WHAT DO AGES MEAN?

Significance of a Measured Thermochronometer Age

A single age from any one thermochronometer has no unique thermal or geological significance. Both the ages that record thermal history and the thermal histories created by geological processes depend on diffusion (since heat flow in the lithosphere is largely controlled by diffusive heat conduction), and nonuniqueness is inherent in diffusive processes. Context is required for even qualitative interpretation of data, usually involving dates from other systems as well as geological information and constraints. If you collaborate with a thermochronologist and they initially ask you what ages you expect, they are not being lazy. They are asking about necessary context. Could there have been reheating? Can nearby unconformities constrain that? What cooling histories are permitted from the tectonic setting?

Two steps are required to take full advantage of thermochronological data: 1) extracting thermal histories from measurements; 2) understanding what those thermal histories might say about geology.

First Step: Thermal-History Modeling

It's usually safe to say a rock was once hot and now it's not, but truly quantitative interpretation of noble gas data requires thermal-history modeling to extract time–temperature histories (as distinct from thermal modeling to predict temperature distributions in geological settings). Given information about sample kinetics and grain size, diffusion models can assess which thermal histories explain measured ages. Forward "what-if" modeling (using trial thermal histories to predict ages) can be a useful first step in examining scenarios. But because of the wide range of possible solutions, this approach is insufficient to explore the full set of solutions. Far better are inverse models that determine the set of thermal histories most consistent with observed ages and geological constraints. Such models can jointly invert mineral-age data as well as $^{40}Ar/^{39}Ar$ and $^{4}He/^{3}He$ release spectra. Those models can also include the impact of accumulated radiation damage on He diffusion kinetics in zircon and apatite such that separate grains from a single sample can be inverted jointly for a segment of thermal history. Codes are available that incorporate most thermochronometers, and they use different approaches that range from simple Monte Carlo searches to efficient learning algorithms. Fox and Shuster (2020 this issue) discuss this approach in more detail.

Second Step: Thermal and Geodynamic Modeling

Determining the nature, timing, and rates of geological processes remains the ultimate rationale for developing thermochronological methods. No single model can handle the complete range of complexity and scale across which these processes occur, but inverse thermokinematic models exist which use key controlling tectonic or geodynamic parameters to explore combinations consistent with the measured thermal evolution (e.g., Braun 2003). This can be done as an independent step, or, ideally, directly combined with thermal-history modeling to create a single integrated inverse model.

HOW CAN AGES BE USED?

Thermochronology has been applied to a wide range of geological environments, driven by creativity about where thermally sensitive tools might be brought to bear and by continuing progress in developing and understanding mineral systems. Examples of this diversity include studies of landscape evolution using natural coal fires (Riihimaki et al. 2009), assessing fault-zone processes or determining the timing of ore deposition (Cooperdock and Ault 2020 this issue), measuring thermal histories for meteorites (Tremblay and Cassata 2020 this issue), and examining thermal histories of various environments in pre-Phanerozoic deep time (McDannell and Flowers 2020 this issue).

Mainstream applications of thermochronology have focused on studies of mountain belts and basins (FIG. 1A and B), including the detrital minerals that link source to sink (FIG. 1B). Basin sediments contain detrital thermochronometers that provide an indirect record of orogenic evolution, and basins themselves can be targets for thermal-history study (Stockli and Naiman 2020 this issue). Because basins host important energy and mineral resources, detailed knowledge of their low-temperature thermal history is important for understanding diagenesis and hydrocarbon maturation. Mountainous regions, whether compressional or extensional in origin, offer rock exposures that record the geodynamic processes responsible for deformation and responding to it, and they have received a large amount of attention over decades (FIG. 1C).

Here, we give just one brief example of an application to an orogen. Other articles in this issue explore at length many of the other applications.

Mountain Building and Landscape Evolution in Tibet

There has been growing interest in understanding how tectonic and Earth-surface processes are coupled, and this work starts with determining the timing and rates of exhumation that occur in response to deformation. Changes in erosion and topography can respond to tectonics at fairly short timescales and wavelengths, especially in areas experiencing rapid landscape evolution. This means that 3-D sampling strategies for thermochronology are important to provide sufficient input to models. One venerable approach exploits age–elevation relationships to estimate the timing and rate of erosion, which works because, in active orogens, older thermochronometer ages are found at higher elevations as a result of those rocks having cooled earlier due to erosion (FIG. 1A).

The study by Tremblay et al. (2015) on southeastern Tibet showcases how integrating multiple thermochronometers, elevation-based sampling, and thermokinematic modeling can reveal just how dynamic and nonintuitive landscape evolution can be across the roof of the world (FIG. 5). Samples taken over 1,100 meters of relief recorded over 300 °C of thermal history spanning 60 Ma. The data document a complex thermal history that includes very rapid cooling between about 17 Ma and 11 Ma, and, of greater interest, almost a total lack of erosional exhumation since then. The best explanation for these data is that deformation shifted into the bordering Himalayan ranges to Tibet's south (Tremblay et al. 2015), causing a reduction in orographic precipitation within Tibet and a significant reorganization of southern Tibet's drainage network. Modeling of alternative scenarios for these data also shows clearly the constraining power and great sensitivity that thermochronology can have (FIG. 5).

FUTURE DIRECTIONS

Thermochronology has a bright future, thanks to both methodological and technological developments. These are leading to new discoveries that expand the range of timescales, temperatures, and processes that we can study, allowing us to ask ever-broader Earth-science questions.

There has been particular interest in developing lower-temperature systems to expand the reach of thermochronology towards shallower environmental conditions, including the study of fluid flow and diagenesis. Exploiting He and Ar diffusion behavior in new minerals such as clays, iron oxides, and hydroxides is promising, as is the $^{40}Ar/^{39}Ar$ dating of illites and the U–Th/He dating of hematite that crystallizes within fault zones. Interest is also growing in hybrid low-temperature methods that exploit the diffusion of cosmogenic nuclides, chiefly ^{21}Ne and ^{3}He.

The accuracy and precision of thermochronometric measurements are currently limited by our kinetic data and our limited knowledge of detailed diffusion mechanisms. Progress will come from further development of *ab initio* calculations to understand 3-D diffusion behavior not only for perfect crystals but also those with different chemistries and classes of imperfections. There will be new experimental studies on real samples that document the impact of various types of imperfections on He diffusion. It is becoming clear that each dated mineral grain represents a unique system with unique diffusion kinetics, meaning that we should expect a range of retentivity for each thermochronometer (FIG. 4). While this might provide the insights needed to explain and manage the excess age dispersion sometimes seen in data sets (Zeitler et al. 2017), cost-effective technical advances are needed to acquire more kinetic data, ideally for all samples. Finally, improvement in inverse codes for thermal-history modeling, integrating more thermochronometers as well as tools for assessing the full uncertainty in thermal histories, would be of great help in getting the most out of the data.

Promising technological innovations are also on the horizon. These include new methods for directly assessing diffusion systematics and for screening samples (Idelman et al. 2018), and new technologies such as laser ablation with higher spatial resolution to directly sample diffusion gradients (Danišík et al. 2017). Finally, because studies often require large sample numbers to constrain complex thermal structures created by topography and tectonics, it will pay to develop cost-effective and rapid analytical methods that can lead to a synoptic thermochronology that addresses larger geographic regions or greater detrital datasets.

ACKNOWLEDGMENTS

Margo Odlum and an anonymous reviewer kindly reviewed this article. PZ acknowledges support from NSF grant EAR-1726350 and CG, support from project RECA-ANR-17-CE01-0012-01.

REFERENCES

Ault AK, Gautheron C, King GE (2019) Innovations in (U–Th)/He, fission track, and trapped charge thermochronometry with applications to earthquakes, weathering, surface-mantle connections, and the growth and decay of mountains. Tectonics 38: 3705-3739

Braun J (2003) Pecube: a new finite-element code to solve the 3D heat transport equation including the effects of a time-varying, finite amplitude surface topography. Computers & Geosciences 29: 787-794

Cooperdock EG, Ault AK (2020) Fe-oxide (U–Th)/He thermochronology: new perspectives on faults, fluids, and heat. Elements 16: 319-324.

Danišík M and 5 coauthors (2017) Seeing is believing: visualization of He distribution in zircon and implications for thermal history reconstruction on single crystals. Science Advances 3, doi: 10.1126/sciadv.1601121

Djimbi DM and 5 coauthors (2015) Impact of apatite chemical composition on (U-Th)/He thermochronometry: an atomistic point of view. Geochimica et Cosmochimica Acta 167: 162-176

Dodson MH (1973) Closure temperature in cooling geochronological and petrological systems. Contributions to Mineralogy and Petrology 40: 259-274

Dodson MH (1986) Closure profiles in cooling systems. Materials Science Forum 7: 145-154

Farley KA (2000) Helium diffusion from apatite: general behavior as illustrated by Durango fluorapatite. Journal of Geophysical Research: Solid Earth 105: 2903-2914

Flowers RM, Ketcham RA, Shuster DL, Farley KA (2009) Apatite (U–Th)/He thermochronology using a radiation damage accumulation and annealing model. Geochimica et Cosmochimica Acta 73: 2347-2365

Fox M, Shuster DL (2020) Lazed and diffused: untangling noble gas thermochronometry data for exhumation rates. Elements 16: 337-342

Gallagher K (2012) Transdimensional inverse thermal history modelling for quantitative thermochronology. Journal of Geophysical Research: Solid Earth 117, doi: 10.1029/2011JB008825

Gautheron C, Tassan-Got L, Barbarand J, Pagel M (2009) Effect of alpha-damage annealing on apatite (U–Th)/He thermochronology. Chemical Geology 266: 157-170

Guenthner WR, Reiners PW, Ketcham RA, Nasdala L, Giester G (2013) Helium diffusion in natural zircon: radiation damage, anisotropy, and the interpretation of zircon (U-Th)/He thermochronology. American Journal of Science 313: 145-198

Guillaume B and 5 coauthors (2013) Dynamic topography control on Patagonian relief evolution as inferred from low temperature thermochronology. Earth and Planetary Science Letters 364: 157-167

Idelman BD, Zeitler PK, McDannell KT (2018) Characterization of helium release from apatite by continuous ramped heating. Chemical Geology 476: 223-232

Ketcham RA (2005) Computational methods for quantitative analysis of three-dimensional features in geological specimens. Geosphere 1: 32-41

Lovera OM, Richter FM, Harrison TM (1991) Diffusion domains determined by ^{39}Ar released during step heating. Journal of Geophysical Research: Solid Earth 96: 2957-2069

McDannell KT, Flowers RM (2020) Vestiges of the ancient: deep-time noble gas thermochronology. Elements 16: 325-330

McDannell KT, Zeitler PK, Janes DG, Idelman BD, Fayon AK (2018) Screening apatites for (U-Th)/He thermochronometry via continuous ramped heating: He age components and implications for age dispersion. Geochimica et Cosmochimica Acta 223: 90-106

McDougall I, Harrisson TM (1999) Geochronology and Thermochronology by the ^{40}Ar/^{39}Ar Method. 2nd Edition. Oxford University Press, Oxford, 269 pp

Reiners PW, Ehlers TA, Zeitler PK (2005) Past, present, and future of thermochronology. Reviews in Mineralogy & Geochemistry 58: 1-18

Reiners PW and 6 coauthors (2018) Geochronology and Thermochronology. John Wiley & Sons, 464 pp

Riihimaki CA, Reiners PW, Heffern EL (2009) Climate control on Quaternary coal fires and landscape evolution, Power River basin, Wyoming and Montana. Geology 37: 255-258

Shuster DL, Farley KA (2004) ^{4}He/^{3}He thermochronometry. Earth and Planetary Science Letters 217: 1-17

Shuster DL, Flowers RM, Farley KA (2006) The influence of natural radiation damage on helium diffusion kinetics in apatite. Earth and Planetary Science Letters 249: 148-161

Stockli DF, Naiman YMR (2020) Detrital Thermochronometry - Recorder of Earth's Dynamic Past. Elements 16: 311-317

Tremblay MM, Cassata WC (2020) Noble gas thermochronology of extraterrestrial materials. Elements 16: 331-336

Tremblay MM and 7 coauthors (2015) Erosion in southern Tibet shut down at ~10 Ma due to enhanced rock uplift within the Himalaya. Proceedings of the National Academy of Sciences of the United States of America112: 12030-12035

Zeitler PK, Brown R, Hackspacher P (2017) Better tools for tracing the thermal history of rocks. Eos 98, doi: 10.1029/2017EO073479

Zeitler PK, Herczeg AL, McDougall I, Honda M (1987) U-Th-He dating of apatite: a potential thermochronometer. Geochimica et Cosmochimica Acta 51: 2865-2868

FIGURES AND FIGURE CAPTIONS

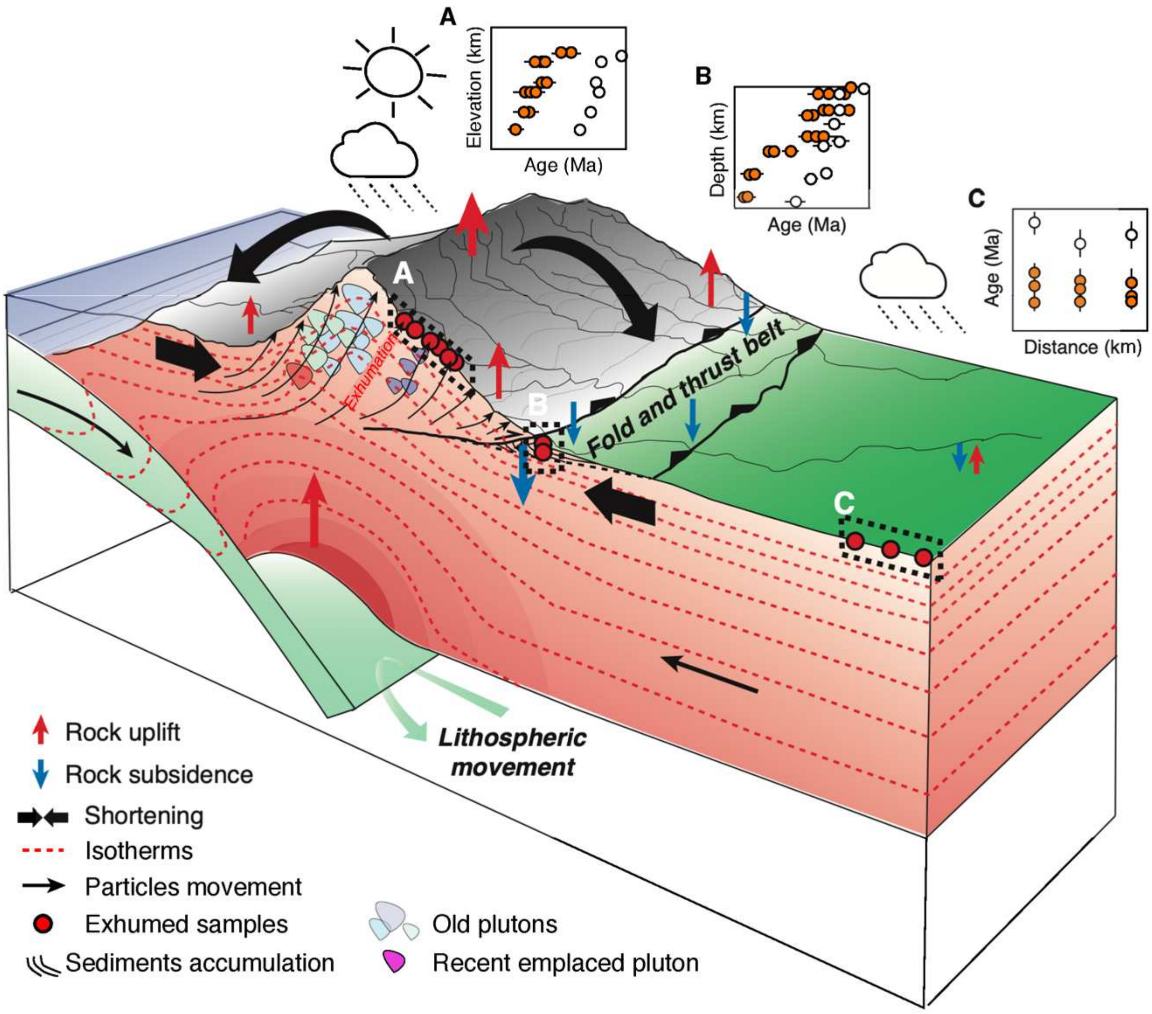

Figure 1 A 3-D block diagram of the isotherm distribution in the crust above an ocean–continent subduction zone, which shows the impact of temperature changes and heat transfer through the lithosphere by pluton emplacement, exhumation, and subsidence and the responses to these processes by erosion, weathering, sediment transport, and sediment accumulation. After Guillaume et al. (2013). (**Inset A**) Representative examples of thermochronometer–ages (Ma) versus elevation (km) of an exhumed mountain. (**Inset B**) Representative examples of thermochronometer ages (Ma) versus depth (km) of rock subsidence across a fold and thrust belt. (**Inset C**) Representative examples of thermochronometer ages (Ma) of basement rocks or detrital sediments verses distance (km) from the rift or mountain belts. For each example, two different systems (1 and 2) with differing closure temperatures (T_c) are shown. System 1 has a lower T_{c1} (filled circles) compared to T_{c2} (open circles)

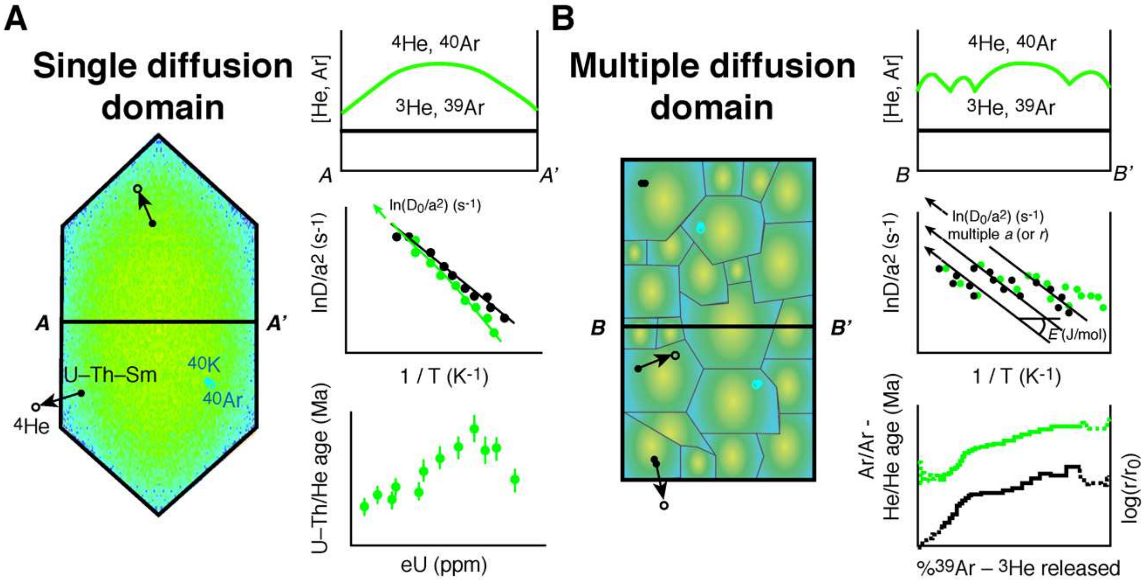

FIGURE 2 A comparison between the diffusion behavior of ^{4}He, ^{3}He and ^{40}Ar, ^{39}Ar in a single crystal and in a multicrystal complex. Symbols: *D* = diffusion coefficient; *a* and *r* refer to the diffusion domain sizes (grain radius or half-width depending on diffusion geometry); eU = effective uranium content. *Ro* = reference apparent radius consistent with the gas release from the smallest diffusion domains. **(A LEFT)** Diffusion behavior of ^{4}He and ^{40}Ar in a single crystal (single diffusion domain) illustrated with the yellow to green to blue color. Transect line marked A-A' relates to data in graphs to right. (**A TOP RIGHT**) ^{4}He, ^{3}He and ^{40}Ar, ^{39}Ar concentration variation along the A-A' transect though the single crystal. As ^{3}He and ^{39}Ar are artificially produced within the crystal by laboratory experiments, the concentration is homogenously distributed, in contrary to ^{4}He and ^{40}Ar concentration. (**A MIDDLE RIGHT**) Evolution of the lnD/a^{2} value as a function of the inverse of the temperature (T) based on the degassed fraction of ^{3}He and ^{4}He from the single crystal. (**A BOTTOM RIGHT**) Example of observed variation of the U–Th/He ages in apatite as a function of the effective uranium content (eU) as presented in (Fig 1A, B and C). (**B LEFT**) Diffusion behavior of ^{4}He and ^{40}Ar in a multicrystal complex (multiple diffusion domain). Colors of yellow to green to blue in each domain (that can be different part of a same crystal or polycrystalline sample) refer to the evolution of ^{4}He and ^{40}Ar concentration with the structure. Transect line marked B-B' relates to data in graphs to right. (**B TOP RIGHT**) ^{4}He, ^{3}He and ^{40}Ar, ^{39}Ar concentration variation along the B-B' transect though the multicrystal. (**B MIDDLE RIGHT**) Evolution of the lnD/a^{2} values as a function of the inverse of the temperature (T) based on the degassed fraction of ^{3}He and ^{4}He from the multicrystal. Note that the diffusion behavior is more complex than for a single crystal (A MIDDLE RIGHT), due to the presence of multi diffusion dimensions (a or r). (**B BOTTOM RIGHT**) Ar/Ar or He/He age spectrum evolution as a function of the % of released ^{39}Ar and ^{3}He content.

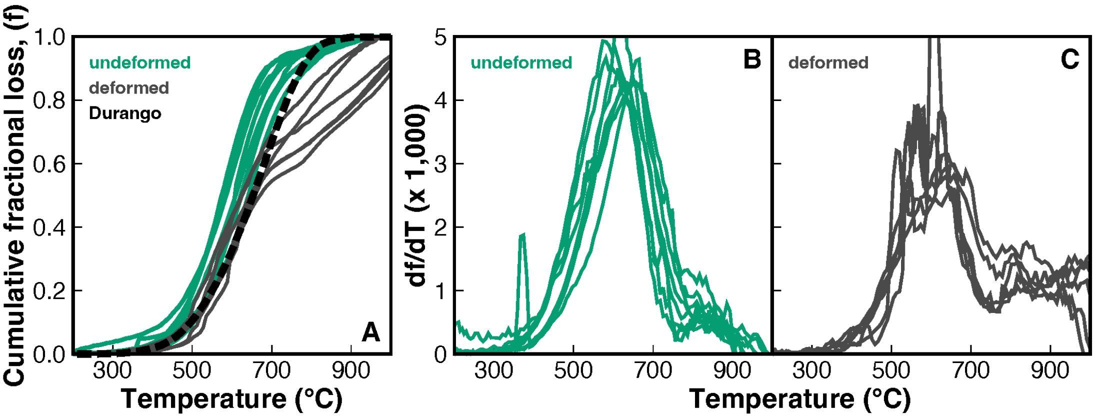

FIGURE 3 Controlled ramped heating data showing incremental ^{4}He release for coeval apatite grains from undeformed and deformed portions of a Sierra Nevada granite. Durango refers to an apatite standard from Durango (Mexico). (**A**) Cumulative ^{4}He release versus temperature. Results from undeformed grains closely match those from the Durango apatite age standard. (**B**) Differential ^{4}He release (derived from data in FIG. 3A) from undeformed apatite grains. Note relatively smooth curve. (**C**) Release of ^{4}He from deformed shear-zones in granite samples. This curve is more irregular than for apatites from the undeformed granite, showing more spikes and including a pronounced high-temperature component that correlates with older ages and greater age dispersion. AFTER MCDANNELL ET AL. (2018).

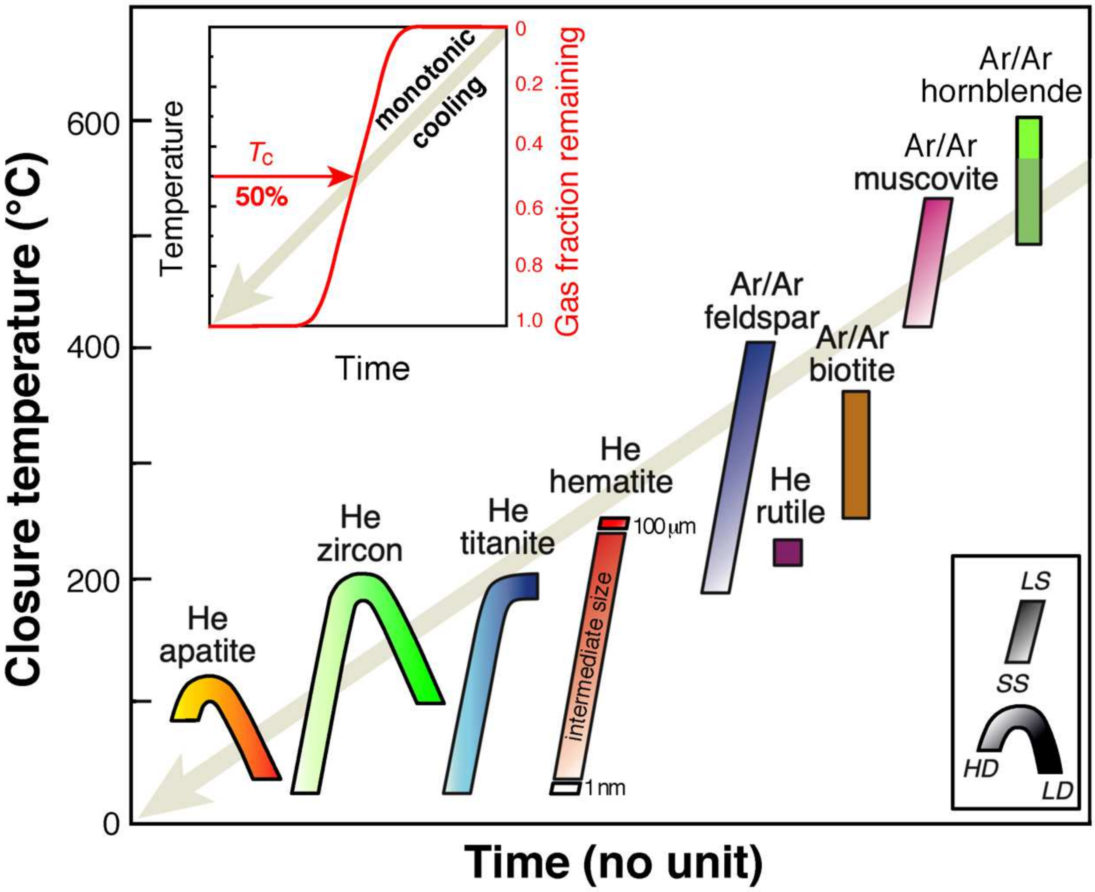

FIGURE 4 The evolution of the closure temperatures (T_c) with time for a range of rock-forming or common accessory minerals used as U–Th/He thermochronometers (apatite, zircon, titanite, hematite, rutile) or $^{40}Ar/^{39}Ar$ thermochronometers (feldspar, biotite, muscovite, hornblende), arranged from lower to higher temperature. (**INSET UPPER LEFT**) Graph of the temperature at which 50% of the radiogenic He or Ar being produced is retained in the crystal (T_c) for a monotonic cooling path. The T_c values correspond to a 10°C/My cooling rate and a 100 μm grain size. (**INSET LOWER RIGHT**) The shape and color gradient of the T_c curves reflect the effects of 1) radiation damage, from low damage (LD) to high damage HD,) and 2) diffusion domain size, from large domain size (LS) to small domain size (SS). For minerals such as apatite, zircon, and titanite, radiation damage alters the He diffusion within the crystal, causing T_c to increase and then decrease again as damage concentration increases and diffusion then inhibits the transition to a more rapid percolation (LD to HD). For samples with multiple diffusion domains (e.g., hematite, feldspar, muscovite), a bulk grain will have a range of T_c values due to the range of different diffusion-domain sizes (LS to SS). The example of hematite presents the Tc value evolution from 100 μm to 1 nm grain size and intermediate value.

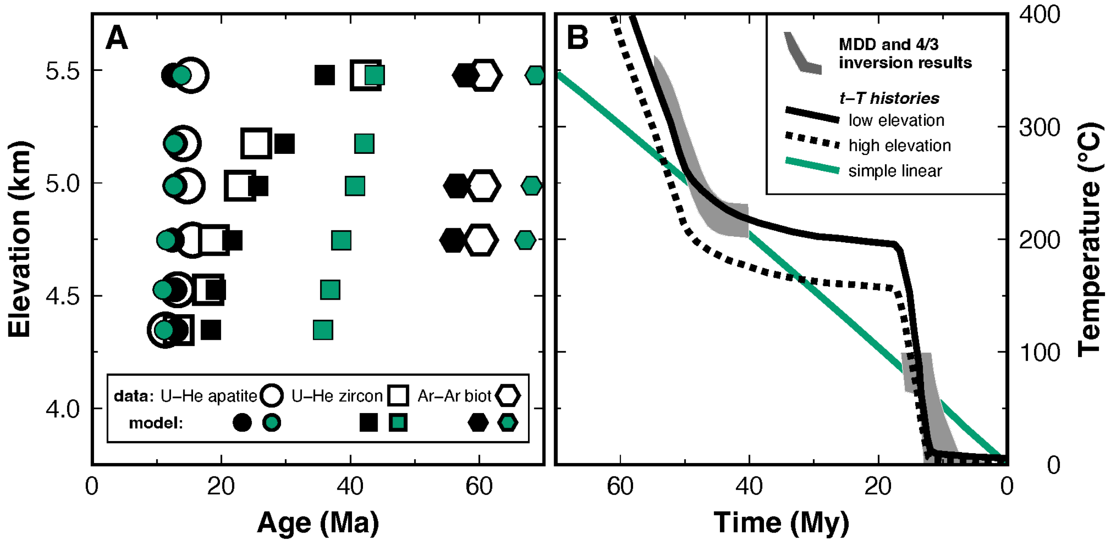

FIGURE 5 Example of thermochronology applied to tectonic-scale landscape evolution in southern Tibet. MDD = multidiffusion domain. (**A**) Observed age–elevation data and predictions from a thermokinematic model that includes landscape evolution. The data are shown by open circles, squares and hexagons; modeled results are filled circles, squares and hexagons, color-coded to match the thermal histories shown in panel (B). (**B**) Thermokinematic models for landscape evolution: a forward model of a simple constant-cooling scenario (straight line decreasing from left to right) and thermal histories for the best-fit inverse model of low- and high-elevation samples. The linear history covers the relevant age and temperature ranges but cannot fit the observed age–elevation relationships, which require a more complex thermal history. The independent $^{40}Ar/^{39}Ar$ MDD K-feldspar and $^{4}He/^{3}He$ apatite inversions (not included in the thermokinematic inversion) agree well with the best-fit model results. AFTER TREMBLAY ET AL. (2015).